

Application of the multiple-scattering method to analysis of systems with semi-infinite photonic waveguides

Wojciech Śmigaj

Surface Physics Division, Faculty of Physics,
Adam Mickiewicz University,
Umultowska 85, 61-614 Poznań, Poland*

We propose a technique of compensating the spurious reflections implied by the multiple-scattering (MS) method, commonly used for analyzing finite photonic crystal (PC) systems, to obtain exact values of characteristic parameters, such as reflection and transmission coefficients, of PC functional elements. Rather than a modification of the MS computational algorithm, our approach involves postprocessing of results obtained by the MS method. We derive analytical formulas for the fields excited in a finite system, taking explicitly into account the spurious reflections occurring at the artificial system boundaries. The intrinsic parameters of the investigated functional element are found by fitting the results of MS simulations to those obtained from the formulas derived. Devices linked with one and two semi-infinite waveguides are analyzed explicitly; possible extensions of the formalism to more complex circuits are discussed as well. The accuracy of the proposed method is tested in a number of systems; the results of our calculations prove to be in good agreement with those obtained independently by other authors.

© 2018 Optical Society of America

OCIS codes: 250.5300, 230.7370, 000.4430, 130.3120.

1. Introduction

Photonic crystals (PCs) have recently become the object of increased interest as possible hosts for optical functional devices, e.g., beam splitters, demultiplexers, etc. [1] These elements, as well as the basic building blocks of photonic integrated circuits—waveguide bends, junctions etc.—have often been investigated by methods designed for finite systems, such as the finite-difference time-domain (FDTD) method [2] and the multiple-scattering (MS) method [3, 4]. Consequently, the devices in question were considered to be embedded in a finite fragment of a PC. This, however, involved spurious reflections at the artificial PC boundaries, significantly complicating the analysis of the device behavior.

To remedy this situation, several methods suitable for analyzing systems with semi-infinite waveguides have been developed. In the effective discrete equations method [5] and the Wannier function method [6], the electric and magnetic fields are represented in a basis of states localized at elementary defects; various grating-based techniques, like those presented in [7, 8, 9], have been developed as well. Both approaches, however, impose some restrictions on the problems to which they can be applied: the former is ill-suited to open systems (i.e., those with vacuum regions extending to infinity), while the latter only applies to systems with uni-

directional waveguides. Recently, the multiple multipole method has been extended by Moreno *et al.* [10] to systems with semi-infinite waveguides; here, the fields on a transverse section of each waveguide, sufficiently distant from discontinuities (junction, bend etc.), are matched to a linear combination of the waveguide eigenstates. As demonstrated in [10], this technique is very general and applicable also to the problems which cannot be dealt by the other above-mentioned methods.

The aim of this paper is to show how to take into account the presence of semi-infinite waveguides in calculations performed on the basis of the MS technique. Owing to its particular simplicity and efficiency in dealing with the case of PCs composed of cylindrical rods, this technique has gained significant popularity [11, 12, 13]. Although the approach proposed by Moreno *et al.* [10] could be straightforwardly carried over to the combination of the MS method and the method of fictitious sources, formulated in [14], this would require significant changes in the computational procedure, as well as availability of externally calculated data describing the fields corresponding to the waveguide eigenstates. In contrast, the approach outlined below consists solely in postprocessing of the results obtained by the ‘pure’ MS method. While admittedly less general than the other technique, it is nevertheless applicable to a number of situations frequently encountered in practice. Two of them are discussed in Sections 2 and 3, in which the proposed procedure is applied to devices linked with one waveguide and two waveguides, respectively. Possible extensions of the method are discussed in Section 4.

*Corresponding author: achu@hoth.amu.edu.pl

2. One waveguide

A. Theory

The first system to be considered is a single waveguide terminated at the surface of a semi-infinite PC [Fig. 1(a)]. A frequently discussed problem (see, e.g., [15, 16, 17]) is the design of the precise shape of the waveguide outlet that would allow maximization of the power transmitted into free space. In this case, the main objective is to calculate the reflection coefficient of the outlet; the intensity of the field produced at some point of the free-space region (possibly at infinity) when an eigenmode of unitary power propagates towards the end of the waveguide is sometimes searched for, too. In the following we will show how both quantities can be found on the basis of calculations done for the finite system shown in Fig. 1(b), presenting a waveguide that is N unit cells long.

The waveguide is assumed to be a single-mode one, and its unit cell to have a mirror-symmetry plane parallel to the yz plane, so that the propagating Bloch states of the waveguide are characterized by wave numbers k and $-k$. An arbitrary source S placed near the waveguide inlet excites the right-propagating mode, which then undergoes multiple reflections. Let u_n and d_n ($n = 0, 1, \dots, N$) denote the z component of the electric (TM polarization) or magnetic (TE polarization) field corresponding to the mode of wave number k and $-k$, respectively, at point n represented by coordinates ($x = na, y = y_0$) in Fig. 1(b). The choice of y_0 is arbitrary; the zero value can be assumed unless the waveguide eigenmode is antisymmetric with respect to the xz plane. From the Bloch theorem, we have

$$\begin{bmatrix} u_n \\ d_n \end{bmatrix} = \hat{T}^n \begin{bmatrix} u_0 \\ d_0 \end{bmatrix}, \quad (1a)$$

$$\begin{bmatrix} u_N \\ d_N \end{bmatrix} = \hat{T}^{N-n} \begin{bmatrix} u_n \\ d_n \end{bmatrix}, \quad (1b)$$

where

$$\hat{T} = \begin{bmatrix} e^{ika} & 0 \\ 0 & e^{-ika} \end{bmatrix} \equiv \begin{bmatrix} \Phi & 0 \\ 0 & \Phi^{-1} \end{bmatrix} \quad (2)$$

is the waveguide transfer matrix; a is the waveguide period and $\Phi \equiv e^{ika}$. The outgoing modes get partly reflected at the waveguide ends; this can be expressed by the following ‘boundary conditions’:

$$d_N = ru_N, \quad (3a)$$

$$u_0 = u_{\text{inc}} + r'd_0, \quad (3b)$$

where r and r' are the reflection coefficients at the waveguide outlet and inlet, respectively, and u_{inc} stands for the effective field corresponding to the right-propagating mode excited by the source S , extrapolated to point $n = 0$. By combining Eqs. (1)–(3) and eliminating the variables u_0 , d_0 , u_N , and d_N , we get the linear system

$$\begin{bmatrix} \Phi^{-n} & -r'\Phi^n \\ r\Phi^{N-n} & -\Phi^{N-n} \end{bmatrix} \begin{bmatrix} u_n \\ d_n \end{bmatrix} = \begin{bmatrix} u_{\text{inc}} \\ 0 \end{bmatrix}, \quad (4)$$

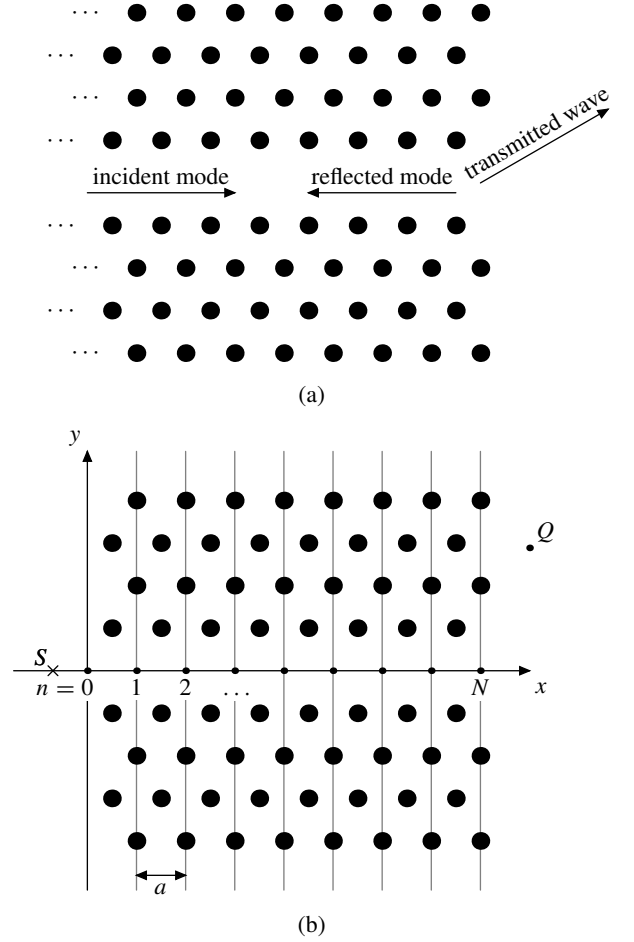


Fig. 1. (a) The ideal system: a semi-infinite waveguide terminated at the surface of a PC. A single mode propagates along the waveguide from inside the PC; on reaching the waveguide outlet, it is partially reflected and partially transmitted into free space. (b) A finite counter-part of the system shown in (a), amenable to analysis by the MS method. The grey lines delimit the N unit cells of the waveguide. Smigaj-1.eps

whose solution reads

$$\begin{bmatrix} u_n \\ d_n \end{bmatrix} = \frac{u_{\text{inc}}}{1 - rr'\Phi^{2N}} \begin{bmatrix} \Phi^n \\ r\Phi^{2N-n} \end{bmatrix}. \quad (5)$$

In cells lying sufficiently far from the waveguide ends for the contribution of the evanescent states to be negligible, the total field f_n can be expressed only in terms of the propagating modes:

$$f_n = u_n + d_n = \frac{\Phi^n + r\Phi^{2N-n}}{1 - rr'\Phi^{2N}} u_{\text{inc}}. \quad (6)$$

We are interested in the reflection coefficient r , as well as in the intensity $|f^{\text{ideal}}(Q)|^2$ of the field which would be generated at some point Q in the free space if the waveguide were semi-infinite and the incident right-propagating mode carried unitary power.

The reflection coefficient can be found simply by least-squares fitting of the numerically calculated values of f_{n+1}/f_n to those calculated by the formula resulting from Eq. (6):

$$\frac{f_{n+1}}{f_n} = \frac{\Phi^{n+1} + r\Phi^{2N-n-1}}{\Phi^n + r\Phi^{2N-n}}. \quad (7)$$

In addition to r , this gives also the value of Φ , which can be used for calculating the wave number k . Let us note by the way that solving Eq. (7) for $n = l - 1$ and $n = l$, where l is some fixed integer, yields

$$k = \pm \frac{1}{a} \arccos \frac{f_{l-1} + f_{l+1}}{2f_l} \quad (8a)$$

and

$$r = \frac{f_{l-1}\Phi - f_l}{f_l\Phi - f_{l-1}}\Phi^{2(l-N)-1}, \quad (8b)$$

these values, calculated for $l \approx N/2$, i.e., near the waveguide center, can be used as starting points in the nonlinear least-squares fitting procedure. The sign of k should correspond to the physics of the problem at hand.

It should be stressed that only cells distant enough from the waveguide ends (i.e., those labeled $n = B, B + 1, \dots, N - B$, where the ‘margin’ B is a sufficiently large integer) should be taken into account in the above fitting procedure, since Eq. (7) has been derived with the assumption that evanescent states are of negligible amplitude in the cells labeled n and $n + 1$.

Let us proceed to the determination of $|f^{\text{ideal}}(Q)|^2$. The intensity $|f(Q)|^2$ of the field generated at point Q in the finite system can be written as

$$|f(Q)|^2 = |t|^2 |\tau(Q)|^2 |u_N|^2 = \frac{|t|^2 |\tau(Q)|^2}{|1 - rr'\Phi^{2N}|^2} |u_{\text{inc}}|^2, \quad (9)$$

where the transmission coefficient $|t|^2 = 1 - |r|^2$ represents the fraction of the total energy emitted into free space when a waveguide mode reaches the outlet, and the ‘transfer coefficient’ $\tau(Q)$, dependent on the position of Q and the geometry of the waveguide outlet, but not on the waveguide length, is a measure of the amount of this energy getting to point Q . In the ideal case of the semi-infinite waveguide, r' would be zero; thus,

$$|f^{\text{ideal}}(Q)|^2 = |t|^2 |\tau(Q)|^2 |u_{\text{inc}}^{\text{ideal}}|^2 \quad (10)$$

with $|u_{\text{inc}}^{\text{ideal}}|^2$ chosen so that the incident mode would carry power $P_{\text{inc}}^{\text{ideal}} = 1$. From Eqs. (9)–(10) we get

$$\begin{aligned} |f^{\text{ideal}}(Q)|^2 &= |1 - rr'\Phi^{2N}|^2 \frac{|u_{\text{inc}}^{\text{ideal}}|^2}{|u_{\text{inc}}|^2} |f(Q)|^2 \\ &= |1 - rr'\Phi^{2N}|^2 \frac{P_{\text{inc}}^{\text{ideal}}}{P_{\text{inc}}} |f(Q)|^2, \end{aligned} \quad (11)$$

since the incident power in each case is proportional to $|u_{\text{inc}}|^2$. As shown in the Appendix, the total power flowing through an arbitrary transverse section of the waveguide is equal to

$$P = \frac{1 - |r|^2}{|1 - rr'\Phi^{2N}|^2} P_{\text{inc}}. \quad (12)$$

This power can be easily calculated by the MS method. By using Eq. (12) for eliminating from Eq. (11) the factor $|1 - rr'\Phi^{2N}|^2$, which contains the unknown coefficient r' , we finally get

$$|f^{\text{ideal}}(Q)|^2 = (1 - |r|^2) \frac{P_{\text{inc}}^{\text{ideal}}}{P} |f(Q)|^2. \quad (13)$$

To sum up, the data obtained in a single MS calculation performed for a finite system with an N -cell-long waveguide suffice for determination of the reflection coefficient of the waveguide outlet, as well as the ‘corrected’ field intensity in free space. When only the former quantity is required, the field excited at $N + 1$ sites lying along the waveguide axis is all that needs to be calculated in the simulation; otherwise, the power flow through an arbitrary transverse section of the finite waveguide must be computed too.

B. Examples

As an example of application of these results, let us first consider the system shown in Fig. 1(a): a W1-type waveguide embedded in a hexagonal lattice of dielectric cylinders with permittivity 11.56 and radius $0.18a$, where a is the lattice constant. The surface termination creates a slight tapering of the waveguide exit. Figure 2 presents the frequency dependence of the reflection coefficient $|r|^2$ in this configuration; the results obtained by the proposed technique are compared to the data reported in [18] [Fig. 7(c)], acquired by the plane-wave-based transfer-matrix method. Our calculations were done for waveguide length $N = 15$ with margin $B = 4$. The convergence is very fast: in fact, the data obtained in the

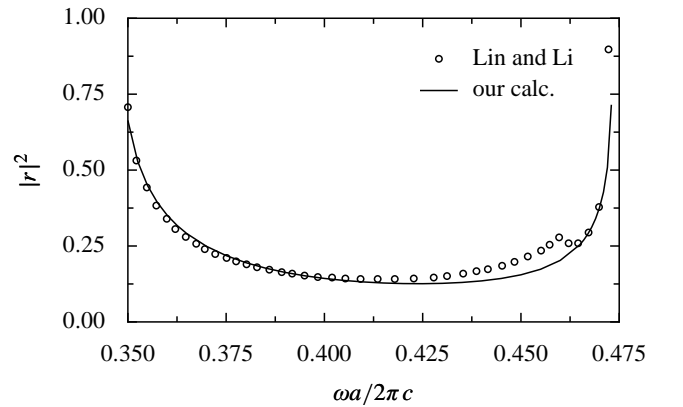


Fig. 2. The reflection coefficient of the waveguide outlet shown in Fig. 1. Circles: the calculation results of Lin and Li [18]; line: results of our calculations. Smigaj-2.eps

$N = 7$, $B = 2$ case (essentially the shortest waveguide for which fitting makes sense) differ by at most 6% from those plotted in the graph, and for frequency values below $0.468 \times 2\pi c/a$ the difference does not exceed 1%. There is a good agreement between our results and those of Lin and Li [18], except for a small peak at frequency value $\omega \approx 0.46 \times 2\pi c/a$, present in the $|r(\omega)|^2$ plot obtained by these Authors, but not reproduced by the curve resulting from our calculations. Since the waveguide is a single-mode one and the mode dispersion curve is smooth around this frequency value, the physical origin of this sharp peak is not clear to us and we believe it might be a numerical artifact.

As a second example, let us consider the leaky-wave photonic antenna [19, 20, 21] shown in Fig. 3(a). Here, the surface surrounding the waveguide outlet is corrugated with period $2a$ and supports leaky surface modes, which are excited by the radiation coming from the waveguide. At a certain frequency value waves scattered at individual perturbed surface cylinders interfere constructively along the surface normal to produce a collimated beam. Figure 3(b) presents the frequency dependence of the far-field intensity of the radiation emitted perpendicularly to the surface; the outcomes of ‘naïve’ calculations done for finite-length waveguides are juxtaposed with those obtained by the proposed scheme for the semi-infinite waveguide. All curves are normalized to their absolute maxima. Evidently, in the finite-waveguide case, the shape of the main peak depends on the precise length of the waveguide; this dependence is especially pronounced to the right of the maximum, where the intensity values obtained for waveguides 11 and 12 cells long differ by as much as a factor of two. On the other hand, the sidelobes in the frequency range $\omega < 0.40 \times 2\pi c/a$ are not significantly affected by changes in the waveguide length; this leads to the conclusion that they result from interference occurring at the crystal surface rather than in the waveguide.

3. Two waveguides

A. Theory

In this Section, we will focus on the more complex system with two linked semi-infinite waveguides; the link can be realized, for instance, by a junction, a bend or a resonant cavity where scattering can occur. Our goal is to calculate the reflection and transmission coefficients of this discontinuity. The waveguides are again assumed to be single-mode ones and to possess a transverse symmetry plane; to these assumptions let us add that of their identical geometry. Figure 4 depicts the finite system used in numerical calculations, where the left and right waveguide comprise N and M unit cells, respectively, and the field is excited by the source S .

Let u_n and d_n denote the field (electric or magnetic, depending on the polarization), at point $n = 0, 1, \dots, N$ inside the left waveguide in Fig. 4, corresponding to the incoming and outgoing guided modes, respectively. Their

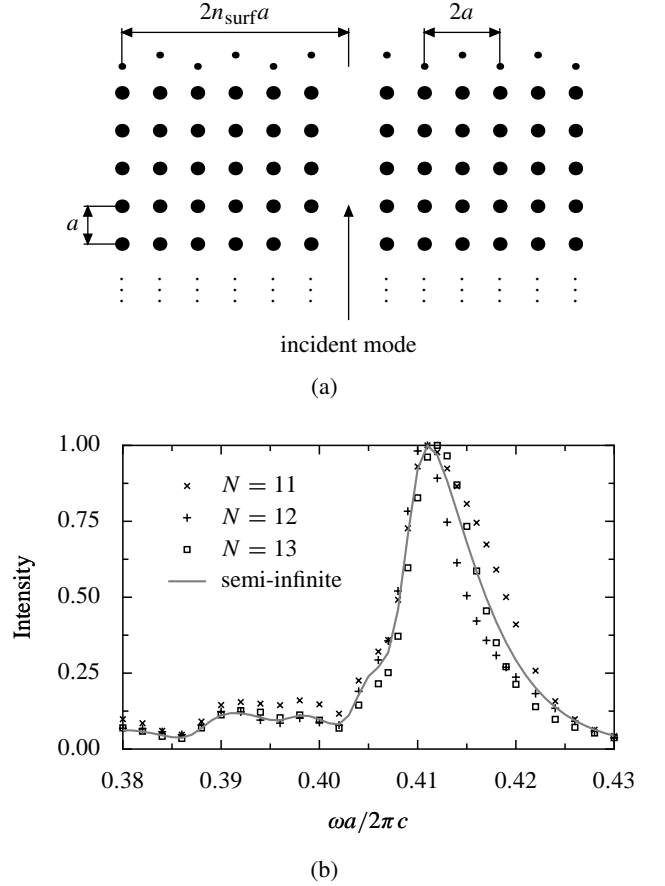


Fig. 3. (a) A photonic crystal leaky-wave antenna. The radii of the bulk and the surface cylinders are $0.18a$ and $0.09a$, respectively, a being the lattice constant; all cylinders have permittivity 11.56. Every second surface cylinder is shifted by $0.3a$ towards the bulk. The corrugated surface is $n_{\text{surf}} = 9$ unit cells long. (b) The far-field intensity of the radiation emitted perpendicularly to the surface, calculated for waveguide length $N = 11, 12$, and 13 , as well as for the semi-infinite waveguide on the basis of data obtained for $N = 12$, $B = 3$. Normalization: see text. Smigaj-3.eps

right-waveguide counterparts at point $m = 0, 1, \dots, M$ will be labeled \bar{u}_m and \bar{d}_m . The junction linking the waveguides can be described by its scattering matrix \hat{S} defined by

$$\begin{bmatrix} d_N \\ \bar{d}_M \end{bmatrix} = \hat{S} \begin{bmatrix} u_N \\ \bar{u}_M \end{bmatrix}, \quad \hat{S} \equiv \begin{bmatrix} \rho & \bar{\tau} \\ \tau & \bar{\rho} \end{bmatrix}; \quad (14)$$

ρ , $\bar{\rho}$ and τ , $\bar{\tau}$ denote the respective reflection and transmission coefficients of the junction. The ‘boundary conditions’ are in this case

$$\bar{u}_0 = r \bar{d}_0, \quad (15a)$$

$$u_0 = u_{\text{inc}} + r d_0, \quad (15b)$$

where r is the reflection coefficient at the waveguide outer ends (the waveguides having the same geometry, their

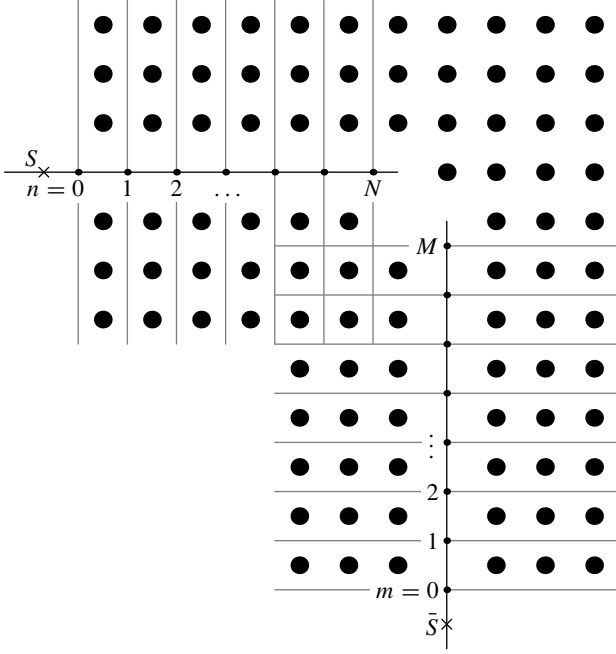


Fig. 4. An example system with two waveguides linked by a junction (in this case, a bend). Grey lines delimit the unit cells of both waveguides. Smigaj-4.eps

terminations can be assumed to be identical too), and u_{inc} is defined as in Section 2. The Bloch theorem gives

$$\begin{bmatrix} u_n \\ d_n \end{bmatrix} = \hat{T}^n \begin{bmatrix} u_0 \\ d_0 \end{bmatrix}, \quad \begin{bmatrix} \bar{u}_m \\ \bar{d}_m \end{bmatrix} = \hat{T}^m \begin{bmatrix} \bar{u}_0 \\ \bar{d}_0 \end{bmatrix}, \quad (16)$$

$$\begin{bmatrix} u_N \\ d_N \end{bmatrix} = \hat{T}^{N-n} \begin{bmatrix} u_n \\ d_n \end{bmatrix}, \quad \begin{bmatrix} \bar{u}_M \\ \bar{d}_M \end{bmatrix} = \hat{T}^{M-m} \begin{bmatrix} \bar{u}_m \\ \bar{d}_m \end{bmatrix}, \quad (17)$$

with the waveguide transfer matrix \hat{T} defined, as before, by Eq. (2). By eliminating the variables u_0, d_0, \bar{u}_0 and \bar{d}_0 from Eqs. (15) and (16), and the variables u_N, d_N, \bar{u}_M , and \bar{d}_M from Eqs. (14) and (17), we obtain the linear system

$$\begin{bmatrix} \Phi^{-n} & -r\Phi^n & 0 & 0 \\ 0 & 0 & \Phi^{-m} & -r\Phi^m \\ \rho\Phi^{N-n} & -\Phi^{-N+n} & \bar{\tau}\Phi^{M-m} & 0 \\ \tau\Phi^{N-n} & 0 & \bar{\rho}\Phi^{M-m} & -\Phi^{-M+m} \end{bmatrix} \begin{bmatrix} u_n \\ d_n \\ \bar{u}_m \\ \bar{d}_m \end{bmatrix} = \begin{bmatrix} u_{\text{inc}} \\ 0 \\ 0 \\ 0 \end{bmatrix}, \quad (18)$$

the solution of which yields the expressions for the total fields in the left and the right waveguides:

$$f_n \equiv u_n + d_n = \frac{(1 - r\bar{\rho}\Phi^{2M})\Phi^n + [\rho + r(\tau\bar{\tau} - \rho\bar{\rho})\Phi^{2M}]\Phi^{2N-n}}{(1 - r\bar{\rho}\Phi^{2M}) - r[\rho + r(\tau\bar{\tau} - \rho\bar{\rho})\Phi^{2M}]\Phi^{2N}} u_{\text{inc}}, \quad (19a)$$

$$\bar{f}_m \equiv \bar{u}_m + \bar{d}_m = \frac{\tau(r\Phi^m + \Phi^{-m})\Phi^{N+M}}{(1 - r\bar{\rho}\Phi^{2M}) - r[\rho + r(\tau\bar{\tau} - \rho\bar{\rho})\Phi^{2M}]\Phi^{2N}} u_{\text{inc}}. \quad (19b)$$

The above procedure can be repeated for the situation when source S is replaced with source \bar{S} located near the entry of the *right* waveguide; in this case, the fields g_n and \bar{g}_m in the left and the right waveguides are given by

$$g_n = \frac{\bar{\tau}(r\Phi^n + \Phi^{-n})\Phi^{N+M}}{(1 - r\rho\Phi^{2N}) - r[\bar{\rho} + r(\tau\bar{\tau} - \rho\bar{\rho})\Phi^{2N}]\Phi^{2M}} \bar{u}_{\text{inc}}. \quad (20a)$$

$$\bar{g}_m = \frac{(1 - r\rho\Phi^{2N})\Phi^m + [\bar{\rho} + r(\tau\bar{\tau} - \rho\bar{\rho})\Phi^{2N}]\Phi^{2M-m}}{(1 - r\rho\Phi^{2N}) - r[\bar{\rho} + r(\tau\bar{\tau} - \rho\bar{\rho})\Phi^{2N}]\Phi^{2M}} \bar{u}_{\text{inc}}, \quad (20b)$$

\bar{u}_{inc} being defined analogously to u_{inc} .

It is important to note that the MS method allows very

efficient calculation of the fields excited in a single structure by several independent sources (e.g., S and \bar{S}), since the scattering matrix of the whole system, whose diagonalization is by far the most time-consuming step of the computational algorithm, is independent of the incident field [3, 4]. In the following we show how the values of f_n, \bar{f}_m, g_n , and \bar{g}_m , calculated by the MS method, can be used for determination of the junction parameters $\rho, \bar{\rho}, \tau$, and $\bar{\tau}$. As before, in all these computations only cells sufficiently distant from the waveguide ends should be taken into account.

1. We have

$$\frac{\bar{f}_{m+1}}{f_m} = \frac{r\Phi^{m+1} + \Phi^{-m-1}}{r\Phi^m + \Phi^{-m}}; \quad (21)$$

therefore, as in the one-waveguide case, the parameters Φ and r can be obtained by least-squares fitting of the above formula's right-hand side to simulation results. Good starting points for the fitting procedure are in this case

$$k = \pm \frac{1}{a} \arccos \frac{\bar{f}_{l-1} + \bar{f}_{l+1}}{2\bar{f}_l} \quad (22a)$$

and

$$r = \frac{\bar{f}_l \Phi - \bar{f}_{l-1}}{\bar{f}_{l-1} \Phi - \bar{f}_l} \Phi^{-2l-1} \quad (22b)$$

with $l \approx M/2$.

2. To shorten the notation, we introduce the following symbols:

$$\mu \equiv r\rho\Phi^{2N}, \quad \bar{\mu} \equiv r\bar{\rho}\Phi^{2M}, \quad (23)$$

$$\nu \equiv r\tau\Phi^{2N}, \quad \bar{\nu} \equiv r\bar{\tau}\Phi^{2M}, \quad (24)$$

$$\zeta \equiv \mu\bar{\mu} - \nu\bar{\nu}, \quad \eta \equiv 1 - \mu - \bar{\mu} + \zeta; \quad (25)$$

consequently, the formulas for f_n , \bar{f}_m , g_n , and \bar{g}_m become:

$$f_n = \frac{(1 - \bar{\mu})\Phi^n + r^{-1}(\mu - \zeta)\Phi^{-n}}{\eta} u_{\text{inc}}, \quad (26a)$$

$$\bar{f}_m = \frac{\nu\Phi^m + r^{-1}\bar{\nu}\Phi^{-m}}{\eta} \Phi^{M-N} u_{\text{inc}}, \quad (26b)$$

$$g_n = \frac{\bar{\nu}\Phi^n + r^{-1}\nu\Phi^{-n}}{\eta} \Phi^{N-M} \bar{u}_{\text{inc}}, \quad (26c)$$

$$\bar{g}_m = \frac{(1 - \mu)\Phi^m + r^{-1}(\bar{\mu} - \zeta)\Phi^{-m}}{\eta} \bar{u}_{\text{inc}}. \quad (26d)$$

Thus, *linear* least-squares fitting of the numerically calculated values of f_n to the function $\alpha_1\Phi^n + \beta_1\Phi^{-n}$ allows to find the coefficients

$$\alpha_1 = \frac{1 - \bar{\mu}}{\eta} u_{\text{inc}}, \quad \beta_1 = \frac{\mu - \zeta}{\eta} \frac{u_{\text{inc}}}{r}. \quad (27a)$$

Similarly, fitting the values of \bar{f}_m , g_n , and \bar{g}_m to the functions $(\alpha_2\Phi^m + \beta_2\Phi^{-m})\Phi^{M-N}$, $(\alpha_3\Phi^n + \beta_3\Phi^{-n})\Phi^{N-M}$, and $\alpha_4\Phi^m + \beta_4\Phi^{-m}$, respectively, yields the values of the coefficients

$$\alpha_2 = \frac{\nu}{\eta} u_{\text{inc}}, \quad \beta_2 = \frac{\bar{\nu}}{\eta} \frac{u_{\text{inc}}}{r}, \quad (27b)$$

$$\alpha_3 = \frac{\bar{\nu}}{\eta} \bar{u}_{\text{inc}}, \quad \beta_3 = \frac{\nu}{\eta} \frac{\bar{u}_{\text{inc}}}{r}, \quad (27c)$$

$$\alpha_4 = \frac{1 - \mu}{\eta} \bar{u}_{\text{inc}}, \quad \beta_4 = \frac{\bar{\mu} - \zeta}{\eta} \frac{\bar{u}_{\text{inc}}}{r}. \quad (27d)$$

3. With definitions (25) of ζ and η included, the formulas for α_1 , β_1 , α_2 , α_3 , α_4 , and β_4 form a system

of six equations with six unknowns: μ , $\bar{\mu}$, ν , $\bar{\nu}$, u_{inc} , and \bar{u}_{inc} . Its solution reads

$$\mu = \frac{r\alpha_4\beta_1 - \alpha_2\alpha_3}{\alpha_1\alpha_4 - \alpha_2\alpha_3}, \quad \bar{\mu} = \frac{r\alpha_1\beta_4 - \alpha_2\alpha_3}{\alpha_1\alpha_4 - \alpha_2\alpha_3}, \quad (28a)$$

$$\nu = \frac{\alpha_2(\alpha_4 - r\beta_4)}{\alpha_1\alpha_4 - \alpha_2\alpha_3}, \quad \bar{\nu} = \frac{\alpha_3(\alpha_1 - r\beta_1)}{\alpha_1\alpha_4 - \alpha_2\alpha_3}, \quad (28b)$$

$$u_{\text{inc}} = \alpha_1 - r\beta_1, \quad \bar{u}_{\text{inc}} = \alpha_4 - r\beta_4. \quad (28c)$$

4. The reflection and transmission coefficients ρ , $\bar{\rho}$, τ , and $\bar{\tau}$ can now be calculated from Eqs. (23)–(24), since the values of all the other parameters are already known.

B. Example

To test the accuracy of our method, we are going to apply it to the waveguide bend depicted in Fig. 4. A number of numerical studies of this system, using different methods, are available in the literature [5, 6, 10], providing a reference for new techniques. The superimposed plot in Fig. 5 shows the frequency dependence of the reflection coefficient $|\rho(\omega)|^2$ (since the bend is symmetric, $\rho = \bar{\rho}$) calculated according to the above-presented scheme against the spectra obtained by the effective discrete equations method [5], the Wannier function method [6], and the multiple multipole method [10]. Clearly, the overall shape of all four curves is very similar, although the exact values of $|\rho(\omega)|^2$ differ, especially near the boundaries of the bulk crystal gap. The spectrum resulting from our calculations is almost identical to that calculated by Moreno *et al.* [10] This may be partly due to the similarity of the MS and multiple multipole methods (in both of them the field is expanded in a basis of Bessel and Hankel functions); however, it must also be noted that these methods are intrinsically ‘exact’ in the sense that the Maxwell equations are solved rigorously, which makes the calculations accuracy only depend on the maximum order of the basis functions kept,

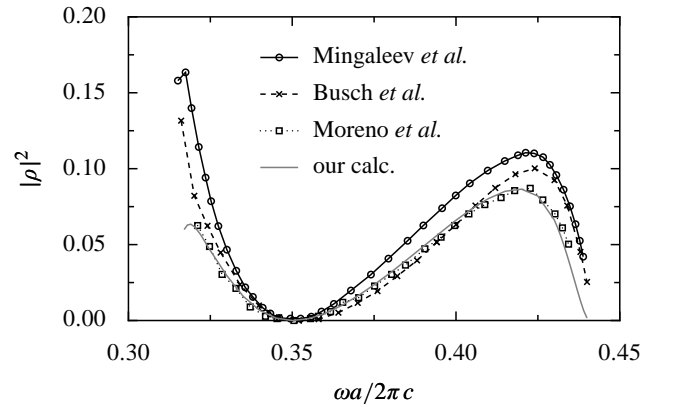


Fig. 5. The reflection coefficient of the bend shown in Fig. 4 calculated by different methods (see text). The data plotted with circles, crosses, and squares have been taken from [5], [6] and [10], respectively. Smigaj-5.eps

and the results are known to be rapidly convergent with the truncation order [4]. In contrast, the derivation of the effective discrete equations [5] involves a number of approximations (for instance, only the monopole eigenmodes of the elementary defects are taken into account). This may be the reason why the reflection coefficient calculated by Mingaleev *et al.* takes values $\sim 30\%$ larger than those obtained in our approach.

4. Extensions

The two device classes discussed above, i.e., those linked with one or two semi-infinite waveguides, represent a large fraction of commonly investigated photonic building blocks. Though the two-waveguide case has been analyzed with the assumption of identical geometry of both waveguides, this condition can be eliminated, with the transmission coefficients renormalized to refer to eigenmodes carrying unitary power, in a way similar to that presented for a single waveguide at the end of Section 2 A.

Our formalism can be extended to systems with more than two waveguides as well. However, many such systems, including most T and Y junctions discussed in the literature, are symmetric with respect to the axis of one or more constituent waveguides. Therefore, they can also be analyzed with the simpler two-waveguide formalism presented in this paper. To see this, note that the scattering matrix \hat{S} of a three-waveguide junction is defined by [cf. Eq. (14)]

$$\begin{bmatrix} d_N^1 \\ d_N^2 \\ d_N^3 \end{bmatrix} = \hat{S} \begin{bmatrix} u_N^1 \\ u_N^2 \\ u_N^3 \end{bmatrix} \quad \text{with} \quad \hat{S} \equiv \begin{bmatrix} \rho_1 & \tau_{21} & \tau_{31} \\ \tau_{12} & \rho_2 & \tau_{32} \\ \tau_{13} & \tau_{23} & \rho_3 \end{bmatrix}, \quad (29)$$

where u_N^i and d_N^i refer to the incoming and outgoing mode, respectively, in the i th waveguide ($i = 1, 2, 3$). For simplicity reasons, all the waveguides are assumed to be of the same length N . If waveguides 2 and 3 are identical and the axis of waveguide 1 is a symmetry plane of the system, we have $\rho_2 = \rho_3$, $\tau_{12} = \tau_{13}$, $\tau_{21} = \tau_{31}$, and $\tau_{23} = \tau_{32}$. To these equalities we can add $u_N^2 = u_N^3$ and $d_N^2 = d_N^3$, provided that the sources are placed symmetrically with respect to that axis. As a result, Eq. (29) simplifies to

$$\begin{bmatrix} d_N^1 \\ d_N^2 \end{bmatrix} = \begin{bmatrix} \rho_1 & 2\tau_{21} \\ \tau_{12} & \rho_2 + \tau_{23} \end{bmatrix} \begin{bmatrix} u_N^1 \\ u_N^2 \end{bmatrix}. \quad (30)$$

Therefore, the junction can be treated as a two-waveguide system with effective reflection and transmission coefficients given by the above formula. The values of these parameters can be calculated by the method presented in Section 3. Evidently, the coefficients ρ_2 and τ_{23} occur only in the form of their sum, and therefore cannot be obtained independently. However, normally, the quantities of interest are the coefficients ρ_1 and τ_{12} , which are related to transmission and reflection of the radiation incoming from the first ('input') waveguide. Equation (30) clearly shows that these parameters can be

obtained straightforwardly from the two-waveguide formalism.

5. Conclusions

We have presented a method, based on multiple-scattering numerical simulations performed for finite systems, allowing to find the reflection and transmission coefficients of photonic crystal functional elements linked with ideal semi-infinite waveguides. As our approach does not involve modification of the existing code implementing the multiple-scattering method, no serious programming and testing effort are necessary for its application. The proposed formalism allows for dealing with a wide variety of photonic crystal building blocks likely to be encountered in practice, as demonstrated by its successful application to a tapered waveguide outlet, a photonic crystal leaky-wave antenna, and a waveguide bend.

Appendix: Power flow in finite waveguides

This Appendix presents the derivation of formula (12) for the power flowing through an arbitrary transverse section of the waveguide shown in Fig. 1(b). Only TM polarization will be considered; the procedure to be followed in the case of TE polarization is completely analogous.

The power $P(na)$ flowing to the right through a plane $x = na$ (perpendicular to the waveguide axis) per unit length in the z direction is given by the integral of the x component of the time-averaged Poynting vector \mathbf{S} :

$$\begin{aligned} P(na) &= \int_{-\infty}^{\infty} S_x dy \\ &= \frac{1}{2} \text{Re} \left[\int_{-\infty}^{\infty} E_z(na, y) H_y^*(na, y) dy \right]. \end{aligned} \quad (A.1)$$

From Eq. (6) we have

$$E_z(na, y) = \frac{\Phi^n + r\Phi^{2N-n}}{1 - rr'\Phi^{2N}} e_z(y), \quad (A.2)$$

where $e_z(y)$ denotes the electric field corresponding to the right-propagating waveguide eigenmode of amplitude satisfying the condition $e_z(0) = u_{\text{inc}}$. Similarly, for the magnetic field we obtain

$$H_y(na, y) = \frac{\Phi^n - r\Phi^{2N-n}}{1 - rr'\Phi^{2N}} h_y(y); \quad (A.3)$$

note the change of sign in the numerator, which results from the magnetic field being a pseudovector. By including these formulas into Eq. (A.1), after some straightforward algebra, we arrive at

$$\begin{aligned} P(na) &= \frac{1}{|1 - rr'\Phi^{2N}|^2} \\ &\times \{ (1 - |r|^2) \text{Re} J - 2 \text{Im}[r\Phi^{2(N-n)}] \text{Im} J \}, \end{aligned} \quad (A.4)$$

where

$$J \equiv \frac{1}{2} \int_{-\infty}^{\infty} e_z(y) h_y^*(y) dy. \quad (\text{A.5})$$

From the conservation of energy, $P(na)$ must be constant for all n , since the waveguide is not leaky. We conclude that the second term in braces in Eq. (A.4), being n -dependent, must be identically zero; this leads to the following condition for the fields corresponding to the waveguide eigenmode:

$$\text{Im } J = 0. \quad (\text{A.6})$$

In consequence, Eq. (A.4) simplifies to

$$P = \frac{1 - |r|^2}{|1 - rr' \Phi^{2N}|^2} P_{\text{inc}}, \quad (\text{A.7})$$

where $P_{\text{inc}} \equiv \text{Re } J$ denotes the power carried by the incident mode.

References

1. L. Thylen, M. Qiu, and S. Anand, “Photonic crystals—a step towards integrated circuits for photonics,” *ChemPhysChem* **5**, 1268–1283 (2004).
2. A. Taflov, *Computational Electrodynamics—The Finite-Difference Time-Domain Method* (Artech-House, 1995).
3. D. Felbacq, G. Tayeb, and D. Maystre, “Scattering by a random set of parallel cylinders,” *J. Opt. Soc. Am. A* **11**, 2526–2538 (1994).
4. G. Tayeb and D. Maystre, “Rigorous theoretical study of finite-size two-dimensional photonic crystals doped by microcavities,” *J. Opt. Soc. Am. A* **14**, 3323–3332 (1997).
5. S. F. Mingaleev and Y. S. Kivshar, “Nonlinear transmission and light localization in photonic-crystal waveguides,” *J. Opt. Soc. Am. B* **19**, 2241–2249 (2002).
6. K. Busch, S. F. Mingaleev, A. Garcia-Martin, M. Schillinger, and D. Hermann, “The Wannier function approach to photonic crystal circuits,” *J. Phys. Cond. Mat.* **15**, R1233–R1256 (2003).
7. L. C. Botten, T. P. White, A. A. Asatryan, T. N. Langtry, C. M. de Sterke, and R. C. McPhedran, “Bloch mode scattering matrix methods for modeling extended photonic crystal structures. I. Theory,” *Phys. Rev. E* **70**, 056606 (2004).
8. T. P. White, L. C. Botten, C. M. de Sterke, R. C. McPhedran, A. A. Asatryan, and T. N. Langtry, “Bloch mode scattering matrix methods for modeling extended photonic crystal structures. II. Applications,” *Phys. Rev. E* **70**, 056607 (2004).
9. Z.-Y. Li and K.-M. Ho, “Light propagation in semi-infinite photonic crystals and related waveguide structures,” *Phys. Rev. B* **68**, 155101 (2003).
10. E. Moreno, D. Erni, and C. Hafner, “Modeling of discontinuities in photonic crystal waveguides with the multiple multipole method,” *Phys. Rev. E* **66**, 036618 (2002).
11. J. Yonekura, M. Ikeda, and T. Baba, “Analysis of finite 2-D photonic crystals of columns and light-wave devices using the scattering matrix method,” *J. Lightwave Technol.* **17**, 1500–1508 (1999).
12. T. Ochiai and J. Sánchez-Dehesa, “Localized defect modes in finite metallic two-dimensional photonic crystals,” *Phys. Rev. B* **65**, 245111 (2002).
13. L.-S. Chen, C.-H. Kuo, and Z. Ye, “Guiding optical flows by photonic crystal slabs made of dielectric cylinders,” *Phys. Rev. E* **69**, 066612 (2004).
14. G. Tayeb and S. Enoch, “Combined fictitious-sources-scattering-matrix method,” *J. Opt. Soc. Am. A* **21**, 1417–1423 (2004).
15. A. Mekis and J. D. Joannopoulos, “Tapered couplers for efficient interfacing between dielectric and photonic crystal waveguides,” *J. Lightwave Technol.* **19**, 861–865 (2001).
16. A. Håkansson, P. Sanchis, J. Sánchez-Dehesa, and J. Martí, “High-efficiency defect-based photonic-crystal tapers designed by a genetic algorithm,” *J. Lightwave Technol.* **23**, 3881–3888 (2005).
17. K. Dossou, L. C. Botten, C. M. de Sterke, R. C. McPhedran, A. A. Asatryan, S. Chen, and J. Brnovic, “Efficient couplers for photonic crystal waveguides,” *Opt. Commun.* **265**, 207–219 (2006).
18. L.-L. Lin and Z.-Y. Li, “Sensitivity to termination morphology of light coupling in photonic-crystal waveguides,” *Phys. Rev. B* **69**, 193103 (2004).
19. E. Moreno, F. J. García-Vidal, and L. Martín-Moreno, “Enhanced transmission and beaming of light via photonic crystal surface modes,” *Phys. Rev. B* **69**, 121402(R) (2004).
20. P. Kramper, M. Agio, C. M. Soukoulis, A. Birner, F. Müller, R. B. Wehrspohn, U. Gösele, and V. Sandoghdar, “Highly directional emission from photonic crystal waveguides of subwavelength width,” *Phys. Rev. Lett.* **92**, 113903 (2004).
21. W. Śmigaj, “A model of light collimation by photonic crystal surface modes,” arXiv:cond-mat/0612652 (2006).